

# Cross-Layer Modeling of Adaptive Wireless Links for QoS Support in Multimedia Networks\*

Qingwen Liu<sup>1</sup>, Shengli Zhou<sup>2</sup> and Georgios B. Giannakis<sup>1</sup>

<sup>1</sup> Dept. of ECE, Univ. of Minnesota, Minneapolis, MN 55455

<sup>2</sup> Dept. of ECE, Univ. of Connecticut, Storrs, CT 06269

## Abstract

Future wired-wireless multimedia networks require diverse quality-of-service (QoS) support. To this end, it is essential to rely on QoS metrics pertinent to wireless links. In this paper, we develop a cross-layer model for adaptive wireless links, which enables derivation of the desired QoS metrics analytically from the typical wireless parameters across the hardware-radio layer, the physical layer and the data link layer. We illustrate the advantages of our model: generality, simplicity, scalability and backward compatibility. Finally, we outline its applications to power control, TCP, UDP and bandwidth scheduling in wireless networks.

## 1. Introduction

Next-generation wired-wireless networks are evolving to accommodate a variety of services, including voice, data and real-time or streaming video/audio. Different applications come with diverse QoS requirements, in terms of data loss, delay and throughput.

The “bottleneck” in such networks is the wireless link, not only because wireless resources (bandwidth and power) are more scarce and expensive than their wired counterparts, but also because the overall system performance degrades markedly due to multipath fading, Doppler, and time-dispersive effects introduced by the wireless air interface. Unlike wired networks, even if large bandwidth/power is allocated to a certain wireless connection, the loss and delay requirements may not be satisfied when the channel experiences deep fades. Therefore, judicious schemes should be developed to support prioritization and resource reservation in wireless networks, in order to enable guaranteed QoS with efficient resource utilization.

To this end, it is essential to construct wireless link models that can provide the desired QoS metrics under diverse

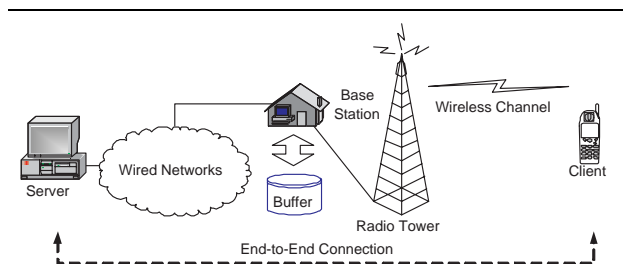


Figure 1. End-to-end connection

wireless conditions. Many models have been established at separate layers, including energy-consumption models for hardware and path-loss models for radio propagation at the hardware-radio layer<sup>1</sup> [7]; the Rayleigh, Rician, Nakagami fading models at the physical layer [20, 22]; and queuing models at the data link layer [5]. These models are suitable for traditional computer or telecommunication networks; however, individually-layered models may not fit future multimedia wireless networks, where QoS support involves radio resource management (RRM), e.g., power control and bandwidth scheduling, across multiple layers. For example, the energy-consumption, path-loss and fading models do not characterize QoS metrics such as delay and buffer overflow; on the other hand, traditional queuing models do not consider typical wireless features, such as power, fading and Doppler effects. These considerations motivate modeling of wireless links for QoS support *across* layers.

In this paper, we develop a cross-layer model of adaptive wireless links for QoS support in multimedia networks. Our model is *distinct* from most existing wireless link models, because it analytically extracts the QoS metrics from the typical wireless parameters across the hardware-radio layer, the physical layer and the data link layer. It offers general-

\* Prepared through collaborative participation in the Communications and Networks Consortium sponsored by the U. S. Army Research Laboratory under the Collaborative Technology Alliance Program, Cooperative Agreement DAAD19-01-2-0011. The U. S. Government is authorized to reproduce and distribute reprints for Government purposes notwithstanding any copyright notation thereon.

<sup>1</sup> The hardware and radio issues could be included in the physical layer. However, theoretical and practical evolution of wireless communications promotes the roles of hardware and radio functions, such as radio frequency (RF) analog circuits, very large scale integration (VLSI) digital circuits, antennas, display equipment, etc.. To improve analysis and design in future wireless communication systems, these functions are preferred to be conceptually isolated from the software or algorithm related physical layer functions, such as modulation and coding, synchronization, training, etc..

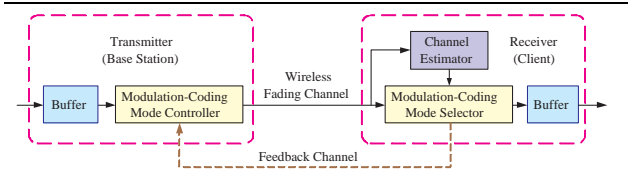


Figure 2. Adaptive wireless link

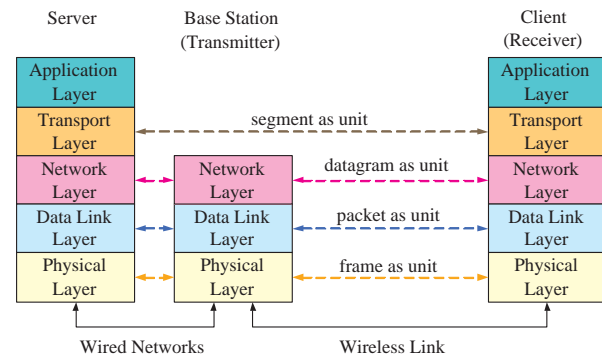


Figure 3. Layers and processing units

ity, simplicity, scalability and backward compatibility.

## 2. Modeling Preliminaries

### 2.1. System Description

Fig. 1 illustrates an end-to-end connection between a server (source) and a client (destination), which includes a wireless link with a single-transmit and a single-receive antenna. As depicted in Fig. 2, a queue (buffer) is implemented at the base station of the wireless link, and operates in a first-in-first-out (FIFO) mode. An adaptive modulation and coding (AMC) controller follows the queue at the base station (transmitter), and the AMC selector is implemented at the client (receiver). The layer structure of the connection under consideration and the processing units at each layer are shown in Fig. 3.

At the wireless link, multiple transmission modes are available, with each mode representing a pair of a specific modulation format, and a forward error correcting (FEC) code, as in the HIPERLAN/2 and the IEEE 802.11a standards [8]. Based on channel estimation at the receiver, the AMC selector determines the modulation-coding pair (mode), which is sent back to the transmitter through a feedback channel, for the AMC controller to update the transmission mode. Coherent demodulation and maximum-likelihood (ML) decoding are employed at the receiver. The decoded bit streams are mapped to packets, which are pushed upward to the data link layer.

We consider the following group of transmission modes: **TM**: Convolutionally coded  $M_n$ -ary rectangular/square

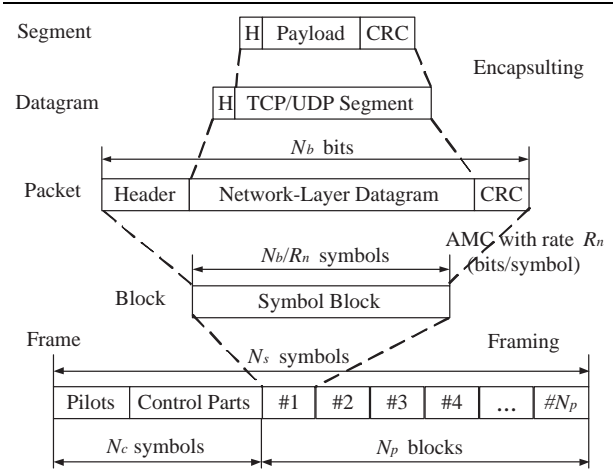


Figure 4. Processing unit at each layer

QAM, adopted from the HIPERLAN/2, or, the IEEE 802.11a standards, which are listed under Table 1, in a rate ascending order.

Although we focus on TM, other transmission modes can be similarly constructed [1–3, 11].

We next detail the processing unit at each layer in Fig. 4:

At the *physical layer* of the wireless link, the data are transmitted frame by frame, where each frame contains a fixed number of symbols ( $N_s$ ). Given a fixed symbol rate, the frame duration ( $T_f$  seconds) is constant, and represents the *time-unit* throughout this paper. With time-division multiplexing (TDM), each frame is divided into  $N_c + N_d$  *time slots*, where for convenience we let each time-slot contain a fixed number of  $N_b/R_1$  symbols. Defining a data packet as a group of  $N_b$  information bits, each time slot can transmit exactly  $R_n/R_1$  packets with transmission mode  $n$ . Specially for the TM, one time-slot can accommodate  $R_1/R_1 = 1$  packet with mode  $n = 1$ ,  $R_2/R_1 = 2$  packets with mode  $n = 2$  and so on. The  $N_c$  time slots contain pilots and control information. The  $N_d$  time slots convey data, which are scheduled to different users with time-division multiple access (TDMA) dynamically. Each user is allocated a certain number of time slots per frame. We focus on a single user here, referring the reader to [17] for scheduling issues of multiple users.

At the *data link layer* of the base station (transmitter), the queue has finite-length (capacity) of  $K$  packets. The queue is served by the AMC module at the physical layer. The customers of the queue are packets.

At the *network layer*, we will not deal with routing issues. At the base station, the arriving process of the datagram stream is assumed to be independent of the AMC and queue status.

At the *transport layer* of the server and the client, the TCP or UDP protocols are implemented,

We next list our operating assumptions:

**A1**: The wireless channel is frequency-flat fading, and remains invariant per frame, but is allowed to vary from frame

	Mode 1	Mode 2	Mode 3	Mode 4	Mode 5
Modulation	BPSK	QPSK	QPSK	16-QAM	64-QAM
Coding Rate $R_c$	1/2	1/2	3/4	3/4	3/4
$R_n$ (bits/sym.)	0.50	1.00	1.50	3.00	4.50
$a_n$	274.7229	90.2514	67.6181	53.3987	35.3508
$g_n$	7.9932	3.4998	1.6883	0.3756	0.0900
$\gamma_{pn}$ (dB)	-1.5331	1.0942	3.9722	10.2488	15.9784

(The generator polynomial of the mother code is  $g = [133, 171]$ .)

**Table 1. Transmission modes with convolutionally coded modulation**

to frame. This corresponds to a block fading channel model, which is suitable for slowly-varying channels. AMC is thus implemented on a frame-by-frame basis [13].

**A2:** Perfect channel state information (CSI) is available at the receiver relying on training-based channel estimation. The corresponding mode selection is fed back to the transmitter without error and latency [4]. The assumption that the feedback channel is error free could be (at least approximately) satisfied by using heavily coding feedback streams. On the other hand, the feedback latency could be compensated by channel prediction [9].

**A3:** If the queue is full, the additional arriving packets will be dropped, so that the overflow content is lost [15].

**A4:** Error detection based on CRC is perfect, provided that sufficiently error detection CRC codes are used [18].

**A5:** If a packet is received incorrectly at the client after error detection, we declare packet loss as well as loss of the encapsulated datagram and segment [16].

For flat fading channels adhering to A1, the channel quality is captured by a single parameter, namely the *instantaneous* received signal-to-noise ratio (SNR)  $\gamma$ . Since the channel varies from frame to frame, we adopt the general Nakagami- $m$  model to describe  $\gamma$  statistically [4]. The received SNR  $\gamma$  per frame is thus a random variable with a Gamma probability density function:

$$p_\gamma(\gamma) = \frac{m^m \bar{\gamma}^{m-1}}{\bar{\gamma}^m \Gamma(m)} \exp\left(-\frac{m\gamma}{\bar{\gamma}}\right), \quad (1)$$

where  $\bar{\gamma} := E\{\gamma\}$  is the *average* received SNR,  $\Gamma(m) := \int_0^\infty t^{m-1} e^{-t} dt$  is the Gamma function and  $m$  is the Nakagami fading parameter ( $m \geq 1/2$ ). This model includes the Rayleigh channel when  $m = 1$ . An one-to-one mapping between the Rician factor and the Nakagami fading parameter  $m$  allows Rician channels to be well approximated by Nakagami- $m$  channels [22].

The wireless channel parameters  $\bar{\gamma}$  and  $m$  are determined by the hardware parameters of wireless equipment (e.g., the transmitter output power  $P_t$ , the receiver noise power  $P_N$ , the antenna loss  $L_i$ ) and by the propagation conditions of radio waves (e.g., the distance between transmitter and receiver  $d$ , the carrier frequency  $f_c$  and the path-loss model).

## 2.2. Adaptive Modulation and Coding (AMC)

Efficient bandwidth utilization for a prescribed error performance at the physical layer can be accomplished with AMC schemes, that match transmission parameters to the wireless channel conditions adaptively and are adopted by many standard wireless networks, such as 3GPP/3GPP2, HIPERLAN/2, IEEE 802.11/15/16 [1–3, 8, 11].

The objective of AMC is to maximize the data rate by adjusting transmission parameters to channel variations, while maintaining a prescribed packet error rate  $P_0$  [4]. Let  $N$  denote the total number of transmission modes available ( $N = 5$  for TM). As in [4], we assume constant power transmission, and partition the entire SNR range in  $N + 1$  non-overlapping consecutive intervals, with boundary points denoted as  $\{\gamma_n\}_{n=0}^{N+1}$ . In this case,

$$\text{mode } n \text{ is chosen, when } \gamma \in [\gamma_n, \gamma_{n+1}). \quad (2)$$

To avoid deep channel fades, no data are sent when  $\gamma_0 \leq \gamma < \gamma_1$ , which corresponds to the mode  $n = 0$  with rate  $R_0 = 0$  (bits/symbol). The design objective of AMC is to determine the boundary points  $\{\gamma_n\}_{n=0}^{N+1}$ .

For simplicity, we approximate the instantaneous packet error rate (PER) as [13, eq. (5)]:

$$\text{PER}_n(\gamma) \approx \begin{cases} 1, & \text{if } 0 < \gamma < \gamma_{pn}, \\ a_n \exp(-g_n \gamma), & \text{if } \gamma \geq \gamma_{pn}, \end{cases} \quad (3)$$

where  $n$  is the mode index,  $\gamma$  is the received SNR, and the mode-dependent parameters  $a_n$ ,  $g_n$ , and  $\gamma_{pn}$  are obtained by fitting (3) to the exact PER<sup>2</sup>. With packet length  $N_b = 1,080$ , the fitting parameters for TM are provided in Table 1 [13]. Based on (1) and (2), the mode  $n$  will be chosen with probability [4, eq. (34)]:

$$\begin{aligned} \text{Pr}(n) &= \int_{\gamma_n}^{\gamma_{n+1}} p_\gamma(\gamma) d\gamma \\ &= \frac{\Gamma(m, m\gamma_n/\bar{\gamma}) - \Gamma(m, m\gamma_{n+1}/\bar{\gamma})}{\Gamma(m)}, \end{aligned} \quad (4)$$

where  $\Gamma(m, x) := \int_x^\infty t^{m-1} e^{-t} dt$  is the complementary incomplete Gamma function. Let  $\overline{\text{PER}}_n$  denote the average PER corresponding to mode  $n$ . In practice, we have

<sup>2</sup> A similar approximation was adopted in [10] but for the bit error rate.

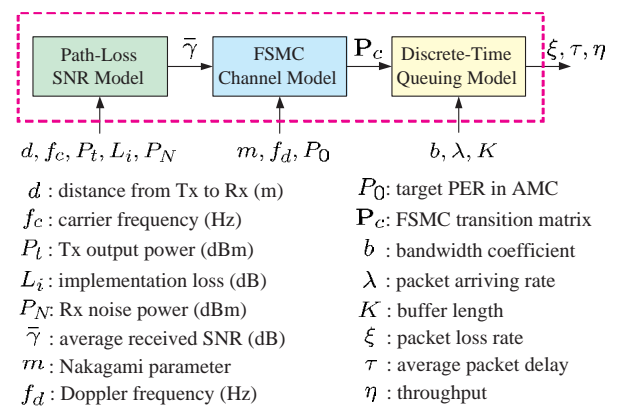


**Figure 5. QoS-oriented wireless link model**

$\gamma_n > \gamma_{pn}$ , which implies that  $\overline{\text{PER}}_n$  can be obtained in closed-form as (c.f. [4, eq. (37)]):

$$\begin{aligned} \overline{\text{PER}}_n &= \frac{1}{\text{Pr}(n)} \int_{\gamma_n}^{\gamma_{n+1}} a_n \exp(-g_n \gamma) p_\gamma(\gamma) d\gamma \quad (5) \\ &= \frac{1}{\text{Pr}(n)} \frac{a_n}{\Gamma(m)} \left( \frac{m}{\bar{\gamma}} \right)^m \frac{\Gamma(m, b_n \gamma_n) - \Gamma(m, b_n \gamma_{n+1})}{(b_n)^m}, \\ & \quad n = 1, \dots, N, \end{aligned}$$

where  $b_n := m/\bar{\gamma} + g_n$ . The average PER of AMC can then be computed as the ratio of the average number of packets in error over the average number of transmitted packets [4]:

$$\overline{\text{PER}} = \frac{\sum_{n=1}^N R_n \text{Pr}(n) \overline{\text{PER}}_n}{\sum_{n=1}^N R_n \text{Pr}(n)}. \quad (6)$$

We want to find the thresholds  $\{\gamma_n\}_{n=0}^{N+1}$ , so that the prescribed  $P_0$  is achieved for each mode:  $\overline{\text{PER}}_n = P_0$ , which naturally leads to  $\overline{\text{PER}} = P_0$  based on (6). Given  $P_0, \bar{\gamma}$ , and  $m$ , the following threshold searching algorithm determines  $\{\gamma_n\}_{n=0}^{N+1}$  and guarantees that  $\overline{\text{PER}}_n$  is exactly  $P_0$  [15]:

**Step 1:** Set  $n = N$ , and  $\gamma_{N+1} = +\infty$ .

**Step 2:** Search for the unique  $\gamma_n \in [0, \gamma_{n+1}]$  based on (5), that satisfies:

$$\overline{\text{PER}}_n = P_0. \quad (7)$$

**Step 3:** If  $n > 1$ , then set  $n = n - 1$  and go to Step 2; otherwise, go to Step 4.

**Step 4:** Set  $\gamma_0 = 0$ .

In summary,  $\{\gamma_n\}_{n=0}^N$  are determined by  $P_0$  in our AMC design. The SNR region  $[\gamma_n, \gamma_{n+1})$  corresponding to transmission mode  $n$  constitutes the channel state indexed by  $n$ . To describe the variation of these channel states, we rely on a finite state Markov chain (FSMC) model, which we detail in the next section.

### 3. QoS-Oriented Wireless Link Model

In this section, we develop a wireless link model across the hardware-radio layer, the physical layer and the data link

layer, which enables us to derive the desired QoS metrics analytically.

Fig. 5 illustrates the wireless link model, which consists of the path-loss SNR, the FSMC channel and the discrete-time queuing sub-modules. The inputs of the model are the wireless link parameters, including channel conditions, radio/hardware resources and traffic characteristics; while the output yields the QoS metrics, i.e., packet loss rate, average packet delay and throughput. We will next specify the model according to these three sub-modules.

#### 3.1. Path-Loss SNR Model

At the hardware-radio layer, the average received SNR  $\bar{\gamma}$  can be expressed as:

$$\bar{\gamma} = P_t - L_i - P_N - L_p, \quad (8)$$

where  $P_t$  (dBm) is the transmitter output power;  $L_i$  (dB) is the implementation loss due to hardware connecting cables, antenna patterns, etc.;  $P_N$  (dBm) is the receiver noise power, which is related to the hardware noise figure and bandwidth [20]; and  $L_p$  (dB) is the path loss due to radio propagation, which is based on many well-established models [20,22]. Here, we adopt the generalized expression of  $L_p$  as:

$$L_p = G_1 + G_2 \log_{10} f_c + G_3 \log_{10} d, \quad (9)$$

where  $G_1, G_2, G_3$  are constants corresponding to application scenarios, e.g., urban or country areas,  $f_c$  (Hz) is the carrier frequency and  $d$  (m) is the distance from transmitter to receiver [20,22].

In summary, given the hardware-radio conditions  $d, f_c, P_t, L_i, P_N$ , the average received SNR  $\bar{\gamma}$  can be determined as in (8), which enables us to characterize the channel variation at the physical layer using the following finite-state Markov chain (FSMC) channel model.

#### 3.2. FSMC Channel Model

The average received SNR  $\bar{\gamma}$  only indicates the large-scale radio propagation characteristics [20,22]. In order to describe small-scale channel variations, we adopt an FSMC channel model as in [21]. Assuming slow fading conditions so that transitions happen only between adjacent states, the probability of transition exceeding two consecutive states is zero [21]; i.e.,

$$P_{l,n} = 0, \quad |l - n| \geq 2. \quad (10)$$

The adjacent-state transition probability can be determined by [21, eqs. (5) and (6)]:

$$\begin{aligned} P_{n,n+1} &= \frac{N_{n+1} T_f}{\text{Pr}(n)}, \quad \text{if } n = 0, \dots, N-1, \\ P_{n,n-1} &= \frac{N_n T_f}{\text{Pr}(n)}, \quad \text{if } n = 1, \dots, N, \end{aligned} \quad (11)$$

where  $N_n$  is the cross-rate of mode  $n$  (either upward or downward), which can be estimated as [24, eq. (17)]:

$$N_n = \sqrt{2\pi \frac{m\gamma_n}{\bar{\gamma}} \frac{f_d}{\Gamma(m)}} \left( \frac{m\gamma_n}{\bar{\gamma}} \right)^{m-1} \exp\left(-\frac{m\gamma_n}{\bar{\gamma}}\right), \quad (12)$$

where  $f_d$  denotes the mobility-induced Doppler spread. The probability of staying at the same state  $n$  is [23]:

$$P_{n,n} = \begin{cases} 1 - P_{n,n+1} - P_{n,n-1}, & \text{if } 0 < n < N, \\ 1 - P_{0,1}, & \text{if } n = 0, \\ 1 - P_{N,N-1}, & \text{if } n = N. \end{cases} \quad (13)$$

Therefore, the transition matrix of the FSMC is banded as:

$$\mathbf{P}_c = [P_{i,j}]_{(N+1) \times (N+1)}. \quad (14)$$

Although we adopted a banded channel transition matrix for simplicity, the ensuing results apply to general channel transition matrices.

In a nutshell, given  $\bar{\gamma}$ ,  $m$ ,  $f_d$ ,  $P_0$  at the physical layer, we model the small-scale channel variations using an FSMC with transition matrix  $\mathbf{P}_c$ , which allows us to derive the QoS metrics of the wireless link at the data link layer through the discrete-time queuing model we outline next.

### 3.3. Discrete-Time Queuing Model

The performance criteria at the physical layer usually exclude delay and overflow. On the other hand, many wireless communication systems operate in discrete-time scales [1–3, 8, 11]. For these reasons, we develop the following discrete-time queuing model to obtain the desired QoS metrics of wireless links.

**3.3.1. Queuing Analysis** Our goal here is to model and analyze the queuing arrival process, the service process and the queue state recursion, in order to derive the stationary behavior of the queuing system along the lines of [15].

With reference to Fig. 6, let  $t$  index time units (frames at the physical layer) and  $A_t$  denote the number of packets arriving in time  $t$ . We assume that the process  $A_t$  is stationary with mean  $E\{A_t\} = \lambda$  and independent of the queue state as well as the channel state. For simplicity, we further assume that  $A_t$  is Poisson distributed with parameter  $\lambda$  (packets/time-unit) [5, pp. 164]:

$$P(A_t = a) = \lambda^a e^{-\lambda} / a!, \quad a \geq 0, \quad (15)$$

where the ensemble-average  $E\{A_t\} = \lambda$  and  $A_t \in \mathcal{A} := \{0, 1, \dots, \infty\}$ .

Different from non-adaptive modulations, AMC dictates a dynamic, rather than deterministic, service process for the queue, capable of transmitting a variable number of packets per time unit (frame). Let  $C_t$  (packets/time-unit) denote this transmission capability, i.e., the number of packets that

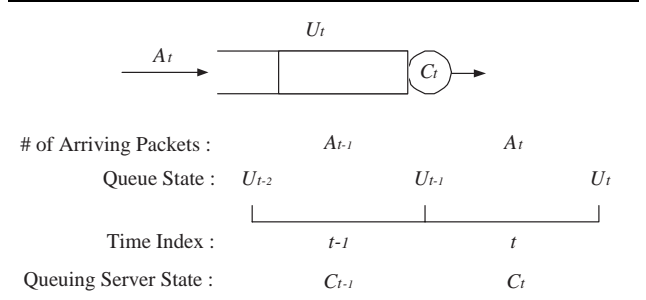


Figure 6. Discrete-time queuing model

can be transmitted at time  $t$ . Corresponding to each transmission mode  $n$ , let  $c_n$  (packets/time-unit) denote the number of packets transmitted with AMC mode  $n$  per time unit. We then have:

$$C_t \in \mathcal{C}, \quad \mathcal{C} := \{c_n : c_n = bR_n/R_1, n = 0, \dots, N\}, \quad (16)$$

where  $b$  is the number of time slots reserved for this connection, that we term *bandwidth coefficient*.

As specified by (16), the AMC module yields a queue server with a total of  $N + 1$  states  $\{c_n\}_{n=0}^N$ , with the service process  $C_t$  representing the evolution of server states. Since the AMC mode  $n$  is chosen when the channel enters the state  $n$ , we model the service process  $C_t$  as an FSMC with transition matrix given by (14).

Having modeled the queue service process, we now focus on the queue itself. Let  $U_t$  denote the queue state (the number of packets in the queue) at the end of time-unit  $t$ , i.e., at the beginning of time-unit  $t + 1$ . It is clear that  $U_t \in \mathcal{U} := \{0, 1, \dots, K\}$ . At time  $t$ , we first transmit  $\min\{U_{t-1}, C_t\}$  packets out of the queue; and have  $A_t$  arriving packets enter the queue. Under the buffer-length constraint  $K$ , we can express the queue state recursion, as in [15, eq. (19)]:

$$U_t = \min\{K, \max\{0, U_{t-1} - C_t\} + A_t\}. \quad (17)$$

In order to obtain the stationary behavior of this queuing system, we construct an FSMC with an augmented state pair  $(U_{t-1}, C_t)$  containing both the queue and the server states. Let  $(U_{t-1}, C_t)$  denote the pair of queue and server states and let  $P_{(u,c),(v,d)}$  denote the transition probability from  $(U_{t-1} = u, C_t = c)$  to  $(U_t = v, C_{t+1} = d)$ , where  $(u, c) \in \mathcal{U} \times \mathcal{C}$  and  $(v, d) \in \mathcal{U} \times \mathcal{C}$ . We can then obtain the transition matrix as (see also [15, eq. (20)]):

$$\mathbf{P} = [P_{(u,c),(v,d)}], \quad (18)$$

having its generic entry given by [15, eq. (22)]:

$$\begin{aligned} P_{(u,c),(v,d)} &= P(U_t = v, C_{t+1} = d | U_{t-1} = u, C_t = c) \\ &= P(C_{t+1} = d | U_t = v, U_{t-1} = u, C_t = c) \\ &\quad \times P(U_t = v | U_{t-1} = u, C_t = c) \\ &= P(C_{t+1} = d | C_t = c) \\ &\quad \times P(U_t = v | U_{t-1} = u, C_t = c), \end{aligned} \quad (19)$$

where the last equality follows from the fact that  $C_{t+1}$  only depends on  $C_t$ , and  $P(C_{t+1} = d|C_t = c) = P_{c,d}$  can be found from the entries of  $\mathbf{P}_c$  in (14). Based on (17), one can easily verify that [15, eq. (23)]:

$$P(U_t = v|U_{t-1} = u, C_t = c) \quad (20)$$

$$= \begin{cases} P(A_t = v - \max\{0, u - c\}) & \text{if } 0 \leq v < K, \\ 1 - \sum_{0 \leq v < K} P(U_t = v|U_{t-1} = u, C_t = c), & \text{if } v = K. \end{cases}$$

We have proved that the stationary (steady-state) distribution of the FSMC  $(U_{t-1}, C_t)$  exists and is unique [15]. Let this stationary distribution be:

$$P(U = u, C = c) := \lim_{t \rightarrow \infty} P(U_{t-1} = u, C_t = c). \quad (21)$$

For notational convenience, let also  $\pi_{(u,c)} := P(U = u, C = c)$ , and define the row vector:

$$\boldsymbol{\pi} := [\pi_{(0,c_0)}, \dots, \pi_{(0,c_N)}, \dots, \pi_{(K,c_0)}, \dots, \pi_{(K,c_N)}]. \quad (22)$$

The stationary distribution of  $(U_{t-1}, C_t)$  can then be computed from the equality [5]:

$$\boldsymbol{\pi} = \boldsymbol{\pi} \mathbf{P}, \quad \sum_{u \in \mathcal{U}, c \in \mathcal{C}} \pi_{(u,c)} = 1, \quad (23)$$

which yields  $\boldsymbol{\pi}$  as the left eigenvector of  $\mathbf{P}$  corresponding to the eigen-value 1. On the other hand, the stationary distribution of  $A_t$  exists as  $t \rightarrow \infty$ . Letting  $A := \lim_{t \rightarrow \infty} A_t$ , from (15), we have:

$$P(A = a) = P(A_t = a), \quad (24)$$

and  $E\{A\} = E\{A_t\} = \lambda$ . Based on the stationary distribution  $P(U = u, C = c)$  and  $P(A = a)$ , it now becomes possible to evaluate the QoS over wireless links as detailed in the following.

**3.3.2. QoS of Wireless Links** Let us now evaluate the QoS metrics in terms of the packet loss rate  $\xi$ , the throughput  $\eta$  and the average delay  $\tau$ , over wireless links. Letting  $P_d$  denote the packet dropping (overflow or blocking) probability upon the queue, and based on  $P(U = u, C = c)$  in (21) and  $P(A = a)$  in (24), we can compute  $P_d$  (c.f. [15, eq. (31)]) as:

$$P_d = \frac{E\{D\}}{E\{A\}} = \frac{E\{D\}}{\lambda}, \quad (25)$$

which is the ratio of the average number of dropping packets  $E\{D\}$  over the average number of arriving packets  $E\{A\}$  per time unit, where

$$E\{D\} = \sum_{a \in \mathcal{A}, u \in \mathcal{U}, c \in \mathcal{C}} \left[ \max\{0, a - K + \max\{0, u - c\}\} \times P(A = a) \times P(U = u, C = c) \right]. \quad (26)$$

A packet is correctly received by the client, only if it is not dropped from the queue (with probability  $1 - P_d$ ) and is correctly received through the wireless channel (with probability  $1 - P_0$ ). Hence, we can obtain the packet loss rate as in [15, eq. (13)]:

$$\xi = 1 - (1 - P_d)(1 - P_0), \quad (27)$$

and the throughput as in [15, eq. (14)]:

$$\eta = E\{A\}(1 - \xi) = \lambda(1 - \xi). \quad (28)$$

Let us now derive the average delay  $\tau$ . With the stationary distribution  $P(U = u, C = c)$  in (21), we can compute the average number of packets in the queue and in transmission as [16, eq. (21)]:

$$N_{wl} = \sum_{u \in \mathcal{U}, c \in \mathcal{C}} u P(U = u, C = c) \quad (29)$$

$$+ \sum_{u \in \mathcal{U}, c \in \mathcal{C}} \min\{u, c\} P(U = u, C = c). \quad (30)$$

Based on Little's Theorem [5], the average delay per packet through the wireless link can be calculated as [16, eq. (22)]:

$$\tau = \frac{N_{wl}}{E\{A\}(1 - P_d)} = \frac{N_{wl}}{\lambda(1 - P_d)}. \quad (31)$$

In summary, given the channel-state transition matrix  $\mathbf{P}_c$ , bandwidth coefficient  $b$ , data arriving rate  $\lambda$  and buffer length  $K$ , we can ascertain QoS over the wireless link analytically through the following steps:

- 1) Construct the FSMC transition matrix  $\mathbf{P}$  of the state pair  $(U_{t-1}, C_t)$  in (18) and compute its stationary distribution  $P(U = u, C = c)$  as in (21).
- 2) Calculate the average number of packets dropped per time-unit  $E\{D\}$  as in (26) and the dropping probability  $P_d$  as in (25).
- 3) Compute the packet loss rate  $\xi$  from (27), the throughput  $\eta$  from (28) and the average packet delay  $\tau$  from (31).

Now, we obtain the QoS metrics of the wireless link  $\xi$ ,  $\tau$ ,  $\eta$ , based on  $\mathbf{P}_c$ ,  $b$ ,  $\lambda$  and  $K$ . We will next discuss the advantages and applications of our QoS-oriented wireless link model.

## 4. Advantages and Applications

### 4.1. Key Advantages

We will next summarize the key advantages of our proposed QoS-oriented wireless link model:

- 1) Generality is offered for analysis and designs of wireless multimedia networks, because the QoS metrics expressed in terms of packet loss rate, average packet delay and throughput can be obtained based on the typical wireless link parameters across the hardware-radio layer, the physical layer and the data link layer.

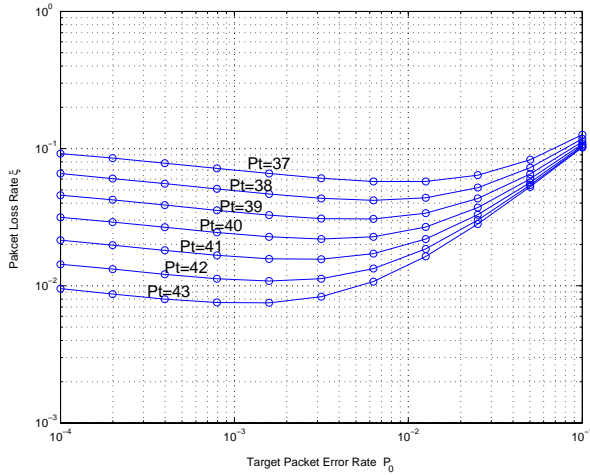


Figure 7. Packet loss rate  $\xi$  vs. target PER  $P_0$

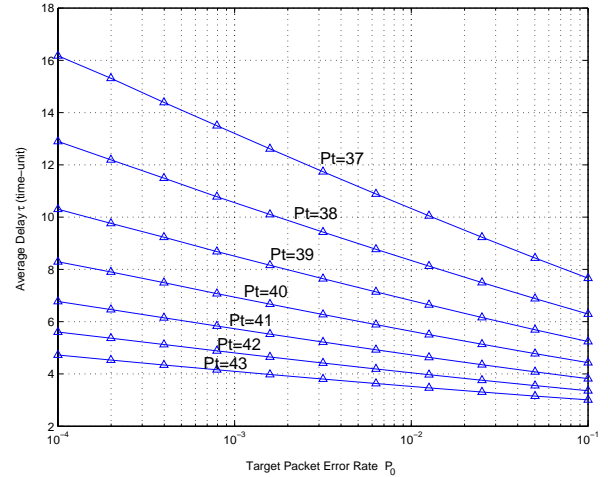


Figure 8. Average delay  $\tau$  vs. target PER  $P_0$

2) Simplicity is provided, because the computational complexity mainly comes from computing the stationary distribution  $\pi$ , that amounts to solving linear equations as in (23). The QoS metrics only need to be updated based on slow-varying parameters. On the other hand, look-up tables can be used in practical implementation.

3) Scalability is ensured, because the three sub-modules, namely the path-loss SNR model, the FSMC channel model and the discrete-time queuing model are isolated, and can thus be individually tailored to fit different scenarios. For example, we may construct the wireless link model by combining the FSMC channel model with the discrete-queuing model, ignoring the intricacies of the hardware-radio layer, as in [14].

4) Backward compatibility is offered, because the path-loss SNR model can be adopted from many well-established radio-propagation models at the hardware-radio layer [20, 22]; the FSMC channel model is widely used in the analysis and designs of wireless networks at the physical layer (c.f., [21] and references therein); and the discrete-time queuing model is based on the standard eigen-decomposition analysis for discrete-time Markov chain at the data link layer [5].

These advantages will be illustrated clearly through the ensuing application examples.

## 4.2. Application Examples

**4.2.1. Power Control for QoS Support** We here illustrate the effect of power control schemes, i.e., varying the transmitter power  $P_t$ , on the QoS metrics of a wireless link.

For the path-loss SNR model, we consider inputs  $d = 800$  (m),  $f_c = 900$  (MHz),  $L_i = 5$  (dB),  $P_N = -100$  (dBm) and let  $P_t$  vary in  $\{37, 38, \dots, 43\}$  (dBm) [20]. We adopt Lee's path-loss model and obtain  $L_p = -130$  (dB) from Fig. 2.46 in [22, pp. 108] for the Philadelphia urban area. Therefore, the average received SNR  $\bar{\gamma}$  is a function of  $P_t$  based on (8). For the FSMC channel model, we assume

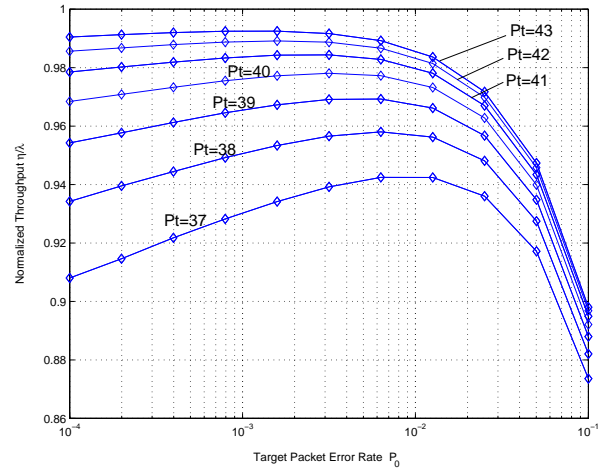


Figure 9. Throughput  $\eta/\lambda$  vs. target PER  $P_0$

$m = 1.0$ ,  $f_d T_f = 0.01$  and  $P_0$  varying over the typical region  $[10^{-4}, 10^{-1}]$ . For the discrete-time queuing model, we suppose  $b = 1$ ,  $\lambda = 2.5$  (packets/time-unit) and  $K = 100$  (packets). Besides, we let  $T_f = 2$  (ms) [8].

We plot the QoS metrics  $\xi$ ,  $\tau$ ,  $\eta/\lambda$  vs.  $P_0$  in Fig. 7, Fig. 8, and Fig. 9 for different values of  $P_t$ . We notice that high transmission power leads to small packet loss rate, low delay and large throughput, because  $\bar{\gamma}$  increases when  $P_t$  becomes large according to (8). For the effects of  $P_0$  on the QoS metrics and the corresponding optimization, we refer the reader to [14–16]. With the extracted QoS metrics, the suitable transmission power can be determined, in order to guarantee the desired QoS with efficient resource utilization.

**4.2.2. TCP Performance in Wireless Access** Based on the reassembled wireless link model with the FSMC chan-

nel and the discrete-time queuing sub-modules, we have also analyzed the performance of TCP protocol in wireless access, using the fixed-point method combining the TCP model [6, 19]; details are reported in [16].

**4.2.3. UDP with QoS Guarantees and Efficient Bandwidth Utilization** In [12], we optimized the bandwidth utilization of an end-to-end UDP connection, guaranteeing the prescribed QoS over adaptive wireless links, based on our reassembled wireless link model.

**4.2.4. Wireless Bandwidth Scheduling in Multiuser Scenario** With the same wireless link model, we developed a bandwidth scheduling algorithm along with an admission control policy, which provides heterogeneous QoS support for multiple users in wireless networks [17].

## 5. Conclusions and Future Directions

In this paper, we developed a cross-layer model of adaptive wireless links for QoS support in multimedia networks. We focused on wireless communication systems with adaptive modulation and coding at the physical layer and finite-length queuing at the data link layer. We then proposed our QoS-oriented wireless link model considering typical wireless link parameters across the hardware-radio layer, the physical layer and the data link layer. We finally illustrated the key advantages of our model (generality, simplicity, scalability and backward compatibility); and outlined its applications to power control, TCP, UDP and bandwidth scheduling in wireless networks.

The frequency-flat fading channels have been studied; however, frequency-selective channels may be considered in the future. Although average packet delay was investigated here, the bounded delay for a given outage probability is under current consideration.

## References

- [1] 3GPP TR 25.848 V4.0.0, *Physical layer aspects of UTRA high speed downlink packet access (release 4)*, 2001.
- [2] 3GPP2 C.S0002-0 Version 1.0, *Physical layer standard for cdma2000 spread spectrum systems*, July 1999.
- [3] IEEE Standard 802.16 Working Group, *IEEE standard for local and metropolitan area networks part 16: air interface for fixed broadband wireless access systems*, 2002.
- [4] M. S. Alouini and A. J. Goldsmith, "Adaptive modulation over Nakagami fading channels," *Kluwer Journal on Wireless Commun.*, vol. 13, no. 1-2, pp. 119–143, May 2000.
- [5] D. Bertsekas and R. Gallager, *Data Networks*, Upper Saddle River, NJ: Prentice-Hall, 2nd Edition, 1992.
- [6] C. F. Chiasserini and M. Meo, "A reconfigurable protocol setting to improve TCP over wireless," *IEEE Trans. on Veh. Tech.*, vol. 51, no. 6, pp. 1608–1620, Nov. 2002.
- [7] S. Cui, A. J. Goldsmith, and A. Bahai, "Energy-constrained modulation optimization for coded systems," in *Proc. of Globecom Conf.*, vol. 1, pp. 372 - 376, San Francisco, CA, Dec. 1-5, 2003.
- [8] A. Doufexi, S. Armour, M. Butler, A. Nix, D. Bull, J. McGeehan, and P. Karlsson, "A comparison of the HIPER-LAN/2 and IEEE 802.11a wireless LAN standards," *IEEE Commun. Mag.*, vol. 40, no. 5, pp. 172–180, May 2002.
- [9] S. Falahati, A. Svensson, T. Ekman, and M. Sternad, "Adaptive modulation systems for predicted wireless channels," *IEEE Trans. on Commun.*, vol. 52, no. 2, pp. 307-316, Feb. 2004.
- [10] K. J. Hole, H. Holm, and G. E. Oien, "Adaptive multidimensional coded modulation over flat fading channels," *IEEE J. on Select. Areas Commun.*, vol. 18, no. 7, pp. 1153–1158, July 2000.
- [11] J. Karaoguz, "High-rate wireless personal area networks," *IEEE Commun. Mag.*, vol. 39, no. 12, pp. 96–102, Dec. 2001.
- [12] Q. Liu, S. Zhou, and G. B. Giannakis, "Efficient bandwidth utilization guaranteeing QoS over adaptive wireless links", in *Proc. of GLOBECOM Conf.*, Dallas, TX, Nov. 29-Dec. 3, 2004.
- [13] Q. Liu, S. Zhou, and G. B. Giannakis, "Cross-layer combining of adaptive modulation and coding with truncated ARQ over wireless links," *IEEE Trans. on Wireless Commun.*, 2004 (to appear).
- [14] Q. Liu, S. Zhou, and G. B. Giannakis, "Queuing with adaptive modulation and coding over wireless links," in *Proc. of MILCOM Conf.*, Boston, MA, Oct. 13-16, 2003.
- [15] Q. Liu, S. Zhou, and G. B. Giannakis, "Queuing with adaptive modulation and coding over wireless links: cross-layer analysis and design," *IEEE Trans. on Wireless Commun.*, 2005 (to appear).
- [16] Q. Liu, S. Zhou, and G. B. Giannakis, "TCP performance in wireless access with adaptive modulation and coding," in *Proc. of Intl. Conf. on Communications*, Paris, France, June 20–24, 2004.
- [17] Q. Liu, S. Zhou, and G. B. Giannakis, "Cross-layer scheduling with predictable QoS guarantees in adaptive wireless networks," *IEEE Journal on Selected Areas in Communications*, 2004 (submitted).
- [18] H. Minn, M. Zeng, and V. K. Bhargava, "On ARQ scheme with adaptive error control," *IEEE Trans. on Veh. Technol.*, vol. 50, no. 6, pp. 1426–1436, Nov. 2001.
- [19] J. Padhye, V. Firoiu, D. F. Towsley, and J. F. Kurose, "Modeling TCP Reno performance: a simple model and its empirical validation," *IEEE/ACM Trans. on Networking*, vol. 8, no. 2, pp. 133–145, Apr. 2000.
- [20] T. Rappaport, *Wireless Communications: Principles and Practice*. Upper Saddle River, NJ: Prentice-Hall Inc., 1996.
- [21] J. Razavilar, K. J. R. Liu, and S. I. Marcus, "Jointly optimized bit-rate/delay control policy for wireless packet networks with fading channels," *IEEE Trans. on Commun.*, vol. 50, no. 3, pp. 484–494, March 2002.
- [22] G. L. Stüber, *Principles of Mobile Communication*. Norwell, MA: Kluwer Academic, 2nd Edition, 2001.
- [23] H. S. Wang and N. Moayeri, "Finite-state Markov channel - a useful model for radio communication channels," *IEEE Trans. on Veh. Tech.*, vol. 44, no. 1, pp. 163–171, Feb. 1995.
- [24] M. D. Yacoub, J. E. Vargas Bautista, and L. G. de R. Guedes, "On higher order statistics of the Nakagami- $m$  distribution," *IEEE Trans. on Veh. Tech.*, vol. 48, no. 3, pp. 790–794, May 1999.
- [25] H. Zhang, "Service disciplines for guaranteed performance service in packet-switching networks," *Proceedings of the IEEE*, vol. 83, no. 10, pp. 1374–1396, Oct. 1995.